

INTERACTION OF STORED, COOLED PROTON BEAMS WITH FIBER TARGETS

B. v. Przewoski, H.O. Meyer, P. Heimberg, W. Lozowski, S.F. Pate,
R.E. Pollock, T. Rinckel, P. Schwandt, F. Sperisen, and W. DeZarn
Indiana University Cyclotron Facility, Bloomington, Indiana 47408

P.V. Pancella

Western Michigan University, Kalamazoo, Michigan 49008

Many target materials that are of interest to nuclear physicists are available only in solid form. Since self-supporting foils are much too thick for use as internal targets, efforts to provide solid targets have utilized schemes where fibers or micro-particles are presented to the stored beam in such a way that the time-averaged thickness is in the desired range. Targets using micron-size particles have been developed,¹ and have been operated successfully in the Indiana Cooler. Like gas targets, they require a substantial technical effort in terms of pumping whereas pumping requirements for fiber targets are much less stringent. An experimental advantage of a fiber target over a gas target is that the luminous volume is well localized. Also, ribbon-shaped fibers present substantially less material to outgoing low-energy recoil particles than dust particles which are at least 1 μm thick.

During the past year we continued our studies of the interaction of stored, cooled proton beams with fiber targets over a range in energy (100-300 MeV). Throughout this study we compared the beam-target interaction for fibers with the performance of a homogeneous gas target of equivalent thickness.

The passage of a beam particle through a relatively thick fiber can be tolerated as long as that particle misses the fiber on many subsequent revolutions, while being cooled on every revolution. In comparison to a gas target where every beam particle intercepts the target on every revolution, heating and cooling are distributed quite differently, and it is not a priori clear that time-averaging results in an inhomogeneous target that is equivalent to a homogeneous gas target.

The manufacturing of 15-20 μm wide and 7-10 $\mu\text{g}/\text{cm}^2$ thick ribbons has become a routine procedure at IUCF.² To further decrease the target thickness, the fiber is moved back and forth across the beam. Thus, the fiber is exposed to the beam only intermittently, which lowers the time-averaged target thickness. The fiber is moved across the beam by mechanically oscillating a frame that holds the fiber.³ Since the time-averaged target thickness is inversely proportional to the amplitude of the oscillation, the target thickness is variable; it is determined from the evaporated thickness, the width of the ribbon, and the amplitude of the oscillation.

In order to separate effects due to the different targets from variations in ring performance, all fiber target measurements were compared to a measurement with a (homogeneous) N_2 gas target. This target was obtained by pressurizing the 16-cm long central region of a differential pumping arrangement which was originally constructed to operate the IUCF gas jet target.⁴

Figure 1 shows 1/e beam lifetime data taken at 6 energies ($T=104, 185, 200, 211, 260$ and 300 MeV) for the oscillating ribbon and the N_2 target. In order to be able to compare

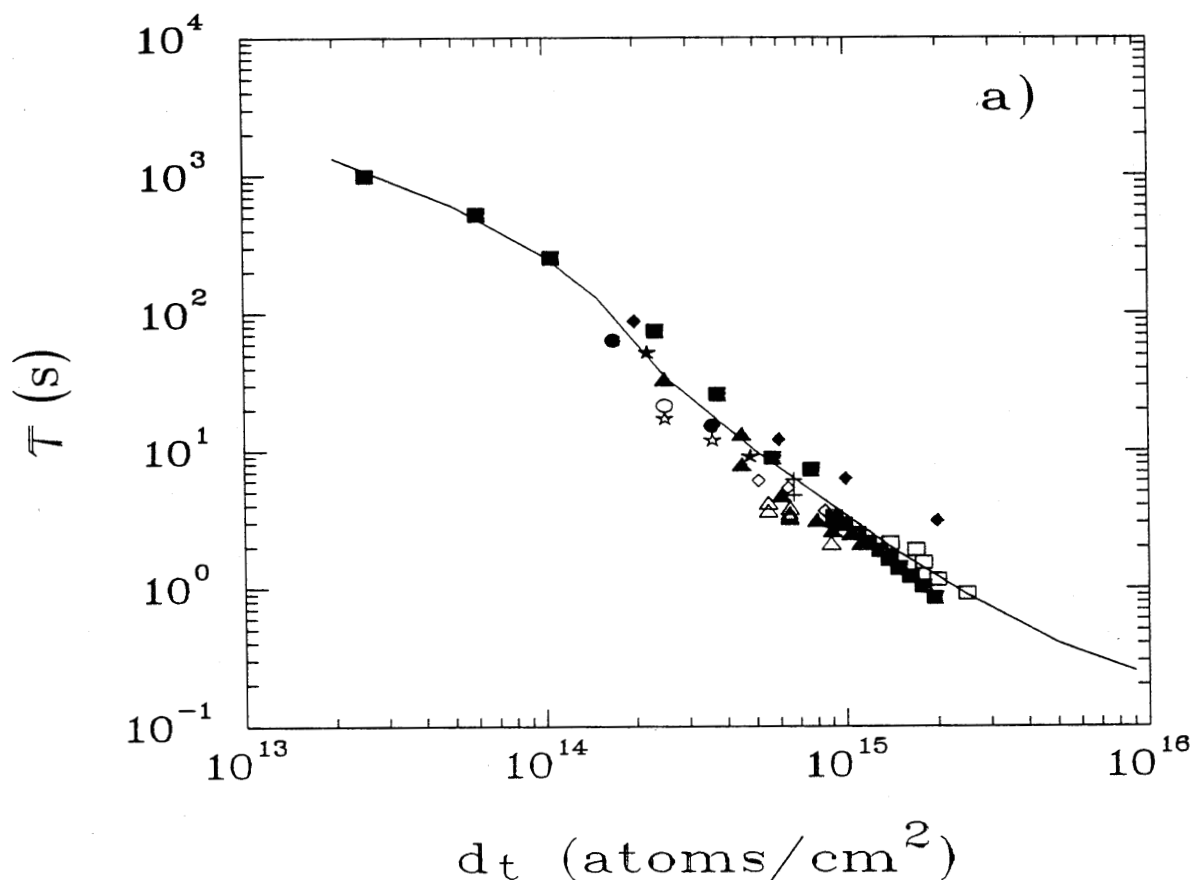


Figure 1. Lifetimes for a carbon ribbon (open symbols) and a N_2 gas target (filled symbols) scaled to 200 MeV, 1.956 MHz and $15\pi \mu\text{m} \cdot \text{rad}$. The data were taken at 104 MeV (crosses), 185 MeV (boxes), 200 MeV (triangles), 211 MeV (diamonds), 260 MeV (circles), and 300 MeV (stars). The curve is a Monte Carlo simulation.

data for different beam energies and machine acceptances, the lifetime is assumed to scale linearly with the machine acceptance and the inverse of the revolution frequency and quadratically with beam energy, since Rutherford scattering is the dominant transverse loss mechanism. Consequently, all data have been scaled to $T_0=200$ MeV, $f_{R_0}=1.956$ MHz and $A_0=15\pi \mu\text{m} \cdot \text{rad}$ by multiplying the measured τ by $(T_0^2 \cdot A_0 / f_{R_0}) / (T^2 \cdot A / f_R)$ where T , f_R and A are beam energy, revolution frequency and acceptance at the time of the measurement. The scatter of the data points is consistent with the uncertainty in measuring the acceptance and the target thickness. The data are to be compared with a Monte Carlo simulation (curve in Fig. 1) at 200 MeV and $15\pi \mu\text{m} \cdot \text{rad}$.³ In principle, one would also expect scaling of the lifetimes by the ratio of their Z^2 values. Since the scatter of the data points is of the same order of magnitude as the ratio of the Z^2 values (1.36) the data have not been scaled according to their Z values and only one curve is shown.

One of the motivations that lead to the construction of the Cooler was the possibility to achieve an extremely small beam energy spread. The Monte Carlo calculation predicts a beam energy spread on the order of a few keV for a coasting beam; somewhat larger values are expected for a bunched beam due to the synchrotron motion of the beam particles inside the RF bucket. The Monte Carlo simulation also predicts that the beam energy spread is the same for a ribbon target as for a gas target of equivalent thickness. To test these predictions of the Monte Carlo code we also studied the beam energy spread in the presence of a target.

The energy spread of a bunched beam was deduced from the distribution of events with respect to the time between the arrival of a scattered proton at a thin scintillator and the occurrence of an RF signal (issued at constant RF phase). Thus this spectrum is related to the spread in phase relative to the RF and therefore to the beam energy spread. For a coasting beam, the energy spread can be deduced from the spread in revolution frequency of the stored particles. This energy spread was measured using a resonant Schottky signal pickup, tuned to a prime multiple of the revolution frequency. No difference in beam energy spread was found when using a ribbon target or a diffuse N₂ target. Figure 2 shows a compilation of all energy spread measurements as a function of target thickness for N₂ (small symbols) and carbon (large symbols) at 185 MeV (dots), 200 MeV (triangles),

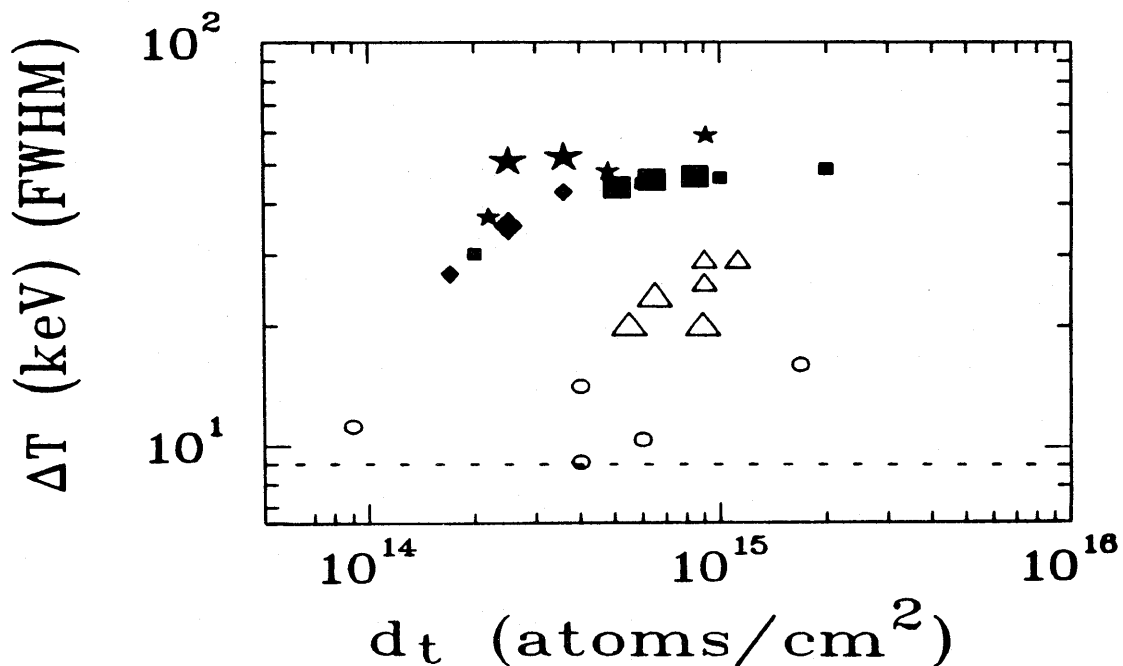


Figure 2. Beam energy spread (FWHM) for bunched beam (solid symbols) and coasting beam (open symbols) as a function of target thickness. The data sample contains data taken with a carbon ribbon (large symbols) and N₂ gas target (small symbols) for coasting and bunched beam at 185 MeV (dots), 200 MeV (triangles), 211 MeV (squares), 260 MeV (diamonds), and 300 MeV (stars). The dotted line corresponds to the beam energy spread without target.

211 MeV (squares), 260 MeV (diamonds) and 300 MeV (stars). The data clearly fall into two groups: the beam energy spread is about a factor of 5 larger for bunched beam (solid symbols) than for coasting beam (open symbols). On the other hand, the energy spread caused by homogeneous or inhomogeneous targets of equivalent thickness is the same within the accuracy of the measurement.

The beam energy spread calculated with the Monte Carlo code for coasting beam on both the $1 \cdot 10^{15} \text{ cm}^{-2}$ thick carbon and the N_2 gas target is only 3.7 keV. It therefore does not agree with the measured values: this is the one aspect in which the computer model fails to reproduce the data. Small energy spreads that have been reported earlier³ could not be reproduced during the course of this experiment. It is at present not known what explains this. One must conclude that there are still important parameters that govern the operation of the Cooler which are not recognized and not controlled.

We found that the beam lifetime and energy spread observed with an oscillating fiber target are in agreement with the same parameters observed with a homogeneous (N_2) target of an equivalent thickness. This was not the case for measurements during the early stages of our studies, when ribbon targets showed shorter lifetimes and wider energy spreads in comparison with a homogeneous target. This effect has subsequently been explained by non-conducting glue joints where the fiber is attached to the frame. For an insulated fiber we measured a lifetime shorter by a factor of about three.

1. H.O. Meyer, A. Berdoz, H. Rohdjess, J. Doskow, F. Sperisen, Nucl. Instr. and Meth. **A295**, 53 (1990).
2. W.R. Lozowski and J.D. Hudson, Proc. 15th World Conf. of the INTDS (Santa Fe, Sept. 1990), Nucl. Instr. and Meth. **A303**, 34 (1991).
3. B. von Przewoski, H.O. Meyer, W. Lozowski, H. Nann, S.F. Pate, R.E. Pollock, T. Rinckel, W.A. DeZarn, H. Rohdjess, W. Scobel, IUCF Sci. and Tech. Rep., May 1990 - April 1991, p. 148.
4. H.O. Meyer, C. Horowitz, H. Nann, P.V. Pancella, S.F. Pate, R.E. Pollock, B. v. Przewoski, T. Rinckel, M.A. Ross, F. Sperisen, Nucl. Phys. **A539**, 633 (1992).